Interference of Wing and Multipropellers

L. TING,* C. H. LIU,† AND G. KLEINSTEIN‡
New York University, Bronx, N.Y.

A systematic procedure is presented for the analysis of the interference of a wing with multipropellers. The assumptions are made that the radius of the propeller and the chord are of the same order and both are much smaller than the span. Using the chord to span ratio as the small expansion parameter, the local two-dimensional solution for the sectional lift to angle-of-attack relationship is uncoupled from the outer three-dimensional solution in the spirit of Prandtl's lifting line theory. Details of the nonuniform stream behind the propellers enter into the local sectional analysis. For the outer solution, the planform of the wing reduces to the lifting line and the stream behind the propellers reduces to a thin sheet of a jet carrying the sectional momentum gained across the propellers and supporting a pressure difference across the sheet. By representing the thin sheet of a jet as a vortex sheet, an integral equation is obtained. When the momentum gain across the propellers is not too large, the integral equation can be further simplified. Several numerical examples are presented to demonstrate the versatility of the analysis.

Introduction

IN the classical analyses[1,2] of the influences exerted by a propeller on a wing, the following assumptions are usually introduced in addition to those for the lifting line theory[3]: 1) the stream behind the propeller is confined inside a circular cylindrical stream tube, 2) the cylindrical propeller stream is extended from upstream infinity ($x = -\infty$) to downstream infinity ($x = \infty$), 3) the velocity U_J inside the propeller stream is uniform, and 4) the relationship between the sectional lift and the angle of attack is based on that of a two-dimensional airfoil in a uniform stream of velocity U_∞ and U_J for sections outside and inside the propeller stream, respectively. These assumptions are shown by the sketches in Fig. 1. Assumptions 1, 2, and 3 are essential for the three-dimensional analysis. Based on assumption 2, the downwash at the lifting line is related to that in downstream infinity, the Trefftz plane. Based on assumption 3, the solution inside as well as that outside the propeller stream are potential solutions. Finally the boundary conditions across the contour dividing these two potential solutions are fulfilled by the use of simple images due to assumption 1.

Attempts to improve the classical analysis were made by replacing the lifting line with the lifting surface using Weissinger's approximation.[4] General formulations were presented for the lifting surface theory.[5] Extension of the classical analysis to non-overlapping multipropellers can be made by accounting for the images and the mutually induced images of a vortex distribution in the Trefftz plane due to each circular jet behind each propeller. The computation is tedious even for two propellers. When the streams behind the propellers partially overlap each other the classical analysis can be carried out in the Trefftz plane after the outer contour of the stream behind the overlapping propellers is mapped into a circle. This represents a generalization of assumption 1. When the contour of the propeller stream is an ellipse analyses are carried out[6,7] by the technique developed for elasticity problems.[8] Solutions for the same problem with an extra restriction that the wing spans the foci of the elliptical contour are given in Ref. 9.

To assess the accuracy of assumption 4, numerical investigations of an airfoil in a two-dimensional nonuniform stream were carried out.[10,11] Figures 2 and 3 illustrate typical results of the analysis. Figure 2 shows the lift variation of a flat plate with chord C at a small angle-of-attack α as a function of the ratio h/C where $2h$ is the sectional height of the propeller stream with uniform velocity U_J submerged in a uniform stream of velocity U_∞. The ratio of the sectional lift with that in a uniform stream of velocity U_∞ increases from unity to $(U_J/U_\infty)^2$ as h/C increases from zero to infinity. The latter limit corresponds to the case when the plate is in a uniform stream of velocity U_J. In a propeller stream, the ratio h/C ranges from zero to at most unity, therefore, the lift ratio is well below $(U_J/U_\infty)^2$ which would be the value implied by assumption 4. Figure 3 shows the lift and angle of attack relationship for a Joukowski profile in a nonuniform stream in the $x-z$ plane with an upstream velocity profile

$$U(z)/U_\infty = 1 + a\exp[-(z/b)^2] \tag{1}$$

This simulates a sectional velocity profile behind a propeller with velocity distribution

$$U(y,z)/U_\infty = 1 + \{[U(0,0) - U_\infty]/U_\infty\}\, e^{-(y^2+z^2)/b^2} \tag{2}$$

where y denotes the spanwise distance from the center of the propeller stream and the exponential decay length b is of the order of the propeller radius. The parameter a in Eq. (1) can

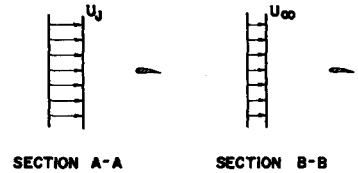

Fig. 1 Schemes for classical analysis.

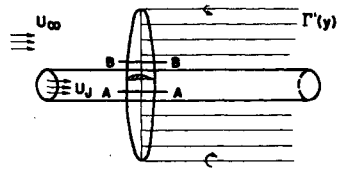

Presented as Paper 71-614 at the AIAA 4th Fluid and Plasma Dynamics Conference, Palo Alto, Calif., June 21–23, 1971; submitted June 30, 1971; revision received February 11, 1972. This research is supported by ARO at Durham.

Index categories: Airplane and Components Aerodynamics; Rotary Wing and VTOL Aerodynamics.

* Professor of Mathematics. Member AIAA.
† Associate Research Scientist.
‡ Research Associate Professor of Aeronautics and Astronautics.

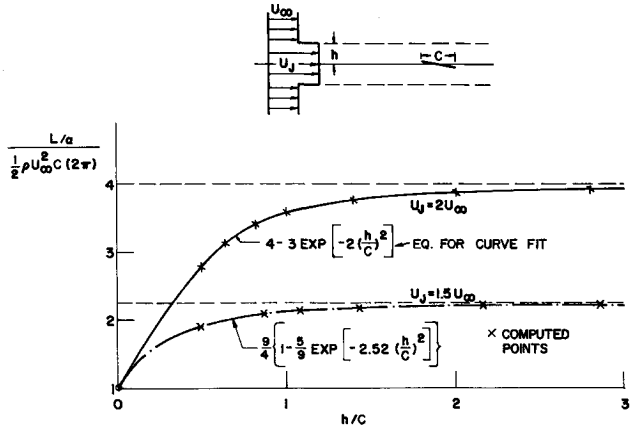

Fig. 2 Effect of sectional height of a propeller stream on the lift for a flat plate.

be identified as $[U(0,0)-U_\infty]/U_\infty \exp[-y^2/b^2]$. At different $x-z$ sections from the center to the outer fringes of the propeller stream, the parameter a takes on various values from $U(0,0)/U_\infty-1$ to zero. In Fig. 3, the mapping circle for the Joukowski profile is centered at $x=-r_0/10$, $z=r_0/10$ with r_0 as its radius. The ratio $U(0,0)/U_\infty$ is chosen to be 2 and the exponential decay length b is equal to $C/1.81$. The two dotted lines in the figure are the lift coefficient curves for the airfoil in a uniform stream of velocity U_∞ and $2U_\infty$, respectively. As shown in the figure the lift coefficient curves for different sections of the propeller stream have different slope and zero angle of attack. Similar to the example in Fig. 2 the lift coefficient curves at different sections in the propeller stream cannot be the same as implied by assumption 4.

This objection to assumption 4 can be overcome by performing the sectional two-dimensional analysis with an appropriate nonuniform upstream velocity distribution. This modification of assumption 4 has been carried out in Ref. 12 and the numerical examples therein demonstrate that the correction due to the modification of the sectional lift characteristics is significant. Furthermore, when the velocity behind is nonuniform, e.g. given by Eq. (2), the surface dividing the propeller stream with the outer stream is not clearly defined. For this case, both assumptions 1 and 3 are violated. Indeed, in the three-dimensional analysis of Ref. 12, it becomes necessary to replace the propeller stream by one fulfilling assumption 1 and 3, i.e., to define with a certain degree of arbitrariness the radius and the mean velocity U_J of the equivalent cylindrical propeller stream.

From previous studies, it is clear that the four assumptions in the classical analysis are justifiable for a single propeller with radius rather large as compared to the chord and placed ahead of the body, i.e., well ahead of the wing. For modern airplanes with multipropellers, the propellers are placed near the wing, their diameters are nearly the same size as the chord and the velocity behind the propellers is not uniform, therefore, the applicability of these four assumptions to wings with multipropellers is in serious question. It is evident that the analysis of the interference of the wing with multipropellers cannot be accomplished by adopting the classical scheme for a single propeller with minor modifications. It is the purpose of this paper to present a new approach to the wing and multipropeller interference problem without relying on any of the aforementioned four assumptions. Simplifications are achieved by utilizing only the fact that the radii of the propellers are of the order of the chord and are much smaller than the span. It is the intention, to be substantiated later, that the proposed analysis will be applicable for any locations of the propellers relative to the wing, for overlapping or nonoverlapping propeller streams and for any velocity distribution behind the propellers which is either uniform with a discontinuity across the surface dividing the propeller stream and the outer stream or is nonuniform and merging smoothly into the outer stream.

In the next section, a new scheme is proposed and the governing equations are derived by relying on physical intuitions in the spirit of Prandtl's lifting line theory. In the subsequent section a systematic expansion scheme is presented with the ratio of the chord to the span as the small parameter. The systematic expansion scheme confirms that the governing equations obtained from physical intuitions are the equations for the leading terms in the asymptotic expansions, shows the condition under which these governing equations can be further simplified and permits the calculation of the higher order terms if required.

Formulation of the Scheme on Physical Intuitions

For modern airplanes with multipropellers, the radii of the propellers are of the order of the chord which is much smaller than the span. Since Prandtl's lifting line theory is formulated on the condition of a small chord to span ratio, some highlights of Prandtl's theory will be restated so that they can be used to guide the formulation of the scheme for the wing and multipropeller interference problem.

Highlights of Prandtl's Lifting Line Theory

In Prandtl's theory, the planform of the wing in the three-dimensional flowfield with the span as the length scale reduces to a line located along the y axis from $y=-S$ to $y=S$. The variations in the sectional geometries of the wing are summarized into one function, the circulation distribution $\Gamma(y)$. The downwash $w(0,y,0)$ induced by the lifting line and its trailing vortex sheet is related to the circulation by the integral equation

$$w(0,y,0)=\frac{1}{4\pi}\int_{-S}^{S}\frac{d\Gamma(\eta)}{y-\eta} \tag{3}$$

where S is the half-span. The circulation at each spanwise station is related to the sectional lift $L(y)$ or the lift coefficient $C_L{}^*$ as follows

$$\Gamma(y)=L(y)/(\rho U_\infty)=\tfrac{1}{2}U_\infty C(y)C_L{}^*(y,\alpha) \tag{4}$$

where $C_L{}^*$ is the lift coefficient of the local airfoil section in a two-dimensional uniform stream at an effective angle of attack $\alpha(y)$. The flow inclination $w(0,y,0)/U_\infty$ at the lifting line is identified as the inclination of the upstream flow in the local

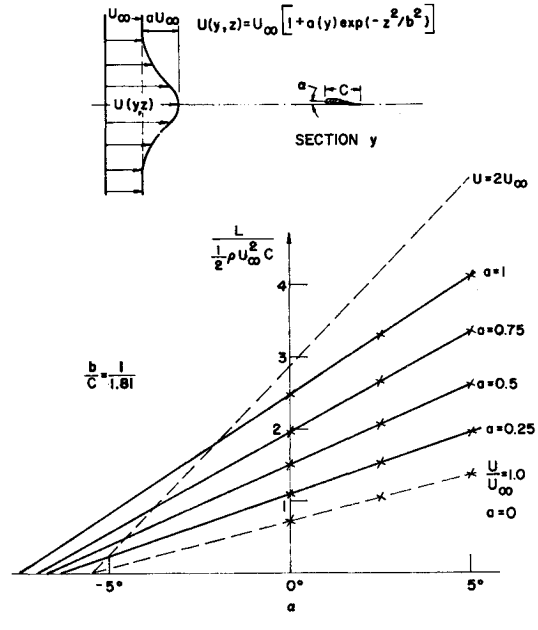

Fig. 3 Sectional lift coefficients for a Joukowski airfoil in a nonuniform stream.

sectional analysis and $\alpha(y)$ is related to the geometrical angle of attack α_g

$$\alpha(y) = \alpha_g(y) - w(0,y,0)/U_\infty \tag{5}$$

the last equation is known as Prandtl's hypothesis. Equations (3–5) are the governing equations for Prandtl's theory. Several points inherent in Prandtl's theory will now be re-emphasized:

a) The solutions are independent of the precise locations of the leading and trailing edges of the wing so long as their distances from the lifting line are of the order of chord and the chord variation $C(y)$ remains unchanged.

b) In the derivation of Eq. (3), the trailing vortex sheet has been assumed to extend from the lifting line downstream along the direction of the undisturbed stream. This assumption which is equivalent to the linearization of the boundary condition, is valid if the inclination of the disturbed stream line is small where the distance from the lifting line is of the order of the span or larger.

c) The theory does not require the assumption of a thin airfoil in the local two-dimensional analysis. Therefore, the disturbed flow inclination near the airfoil, i.e., of the order of the chord, can be finite. The theory requires only the knowledge of the sectional lift coefficient $C_L{}^*(y,\alpha)$. There are methods available for the determination of $C_L{}^*$ for an airfoil section of finite thickness at finite angle of attack or with a flap at a finite deflection angle, namely, the method of conformal mapping or two-dimensional numerical analysis. Of course, the determination of $C_L{}^*(y,\alpha)$ can be much more tedious than the solution of the lifting line equations, Eqs. (3–5).

Scheme for the Wing and Multipropeller Interference Problem

In Prandtl's theory, the planform reduces to the lifting line as the limit of the chord to span ratio approaches zero. In the same spirit, the effective height of the stream behind the propeller, which is of the order of the chord, reduces to zero as compared to the span. On the other hand, the total spanwise spread of the streams behind all the propellers can be of the order of the span. For propellers placed ahead, behind or in the middle of the wing, the horizontal distance x_p from a propeller disk to the lifting line and the vertical distance between the axis of a propeller and the lifting line will both be at most of the order of the chord and equal to zero in the scale of the span. Consequently, the propeller streams reduce to a thin sheet extending from the lifting line backward in the same plane as the trailing vortex sheet as shown in Fig. 4. Because of the momentum gain across the propeller disk the velocity distribution inside the propeller streams will differ from the outer undisturbed velocity by a finite amount. The thin sheet of the propeller streams is therefore equivalent to a thin sheet of a jet carrying a momentum $J(y)$ per unit span equal to the sectional momentum gain across the propeller disk, i.e.,

$$J(y) = \rho \int_{-\infty}^{\infty} [U(y,z) - U_\infty] U(y,z)\, dz \tag{6}$$

$U(y,z)$ is the velocity distribution behind the propellers. The integral involves the momentum difference instead of the momentum because the integral in Eq. (6) balances the sectional thrust force across the propeller disks.

Because of the momentum $J(y)$ carried by the thin sheet, the bending of the sheet implies a change in vertical momentum which has to be balanced by the pressure across the sheet. Their relationship is

$$\Delta p = p(x,y,0^+) - p(x,y,0^-) = -J\theta_x(x,y,0) \tag{7}$$

where θ at $z=0$ is the inclination of the sheet. The pressure difference can be related to the x component of the disturbance velocity outside of the thin sheet by means of the linearized Bernoulli's equation

$$\Delta p = -\rho U_\infty [u(x,y,0^+) - u(x,y,0^-)] \tag{8}$$

The jump in u across the thin sheet is equivalent to a vorticity distribution of surface density $\gamma(x,y)$ which is now related to the curvature of the sheet through Eqs. (7) and (8) as follows

$$\gamma(x,y) = -\Delta p/(\rho U_\infty) = J\theta_x(x,y,0) \tag{9}$$

Since the flow inclination is continuous across the thin sheet of the propeller streams while the downwash, which is equal to the inclination times $U(y,z)$, does not have a limit at the thin sheet, it is desirable in the present problem to work with the flow inclination instead of the downwash. The flow inclination is related to the surface vorticity distribution and the circulation along the lifting line by the following integral relationship:

$$\theta(x,y,z) = \int_{-s}^{s} G(x,y-\eta,z)\Gamma'(\eta)\, d\eta + \int_{-\infty}^{\infty} G(x,y-\eta,z)\Gamma_J'(\eta)\, d\eta + \int_0^\infty d\xi \int_{-\infty}^{\infty} d\eta\, G(x-\xi,y-\eta,z)\gamma_\eta(\xi,\eta) \tag{10}$$

where

$$G(x,y,z) = \frac{1}{4\pi U_\infty}\left\{\frac{y}{y^2+z^2} + \frac{xy}{[x^2+y^2+z^2]^{1/2}} \times \left[\frac{1}{x^2+z^2} + \frac{1}{y^2+z^2}\right]\right\}$$

The circulation $\Gamma_J(y)$ is the contribution of the sectional force $\rho U_\infty \Gamma_J(y)$, required to deflect the propeller momentum to the local inclination, i.e.,

$$\Gamma_J(y) = -J(y)\theta(0,y,0)/(\rho U_\infty) \tag{11}$$

Both Γ_J and γ are proportional to the momentum $J(y)$, therefore, the spanwise integrations in the second and third integrals in Eq. (10) will be restricted to the interval where $J(y) \neq 0$.

The circulation $\Gamma(y)$ is related to the sectional lift of the airfoil or to the lift coefficient C_L as follows

$$\Gamma(y) = L(y)/(\rho U_\infty) = \tfrac{1}{2} U_\infty\, C(y) C_L(y,\alpha) \tag{12}$$

The effective angle of attack $\alpha(y)$ is now related to the geometrical angle of attack and the inclination $\theta(0,y,0)$,

$$\alpha(y) = \alpha_g(y) - \theta(0,y,0) \tag{13}$$

Equation (13) is equivalent to Eq. (5) in Prandtl's theory.

At a section outside the propeller streams, the lift coefficient C_L in Eq. (12) is determined in the same manner as in Prandtl's theory in Eq. (4). At a section y_0 inside the propeller streams, the lift coefficient $C_L(y_0,\alpha)$ will be obtained from the analysis of the airfoil section in a two-dimensional nonuniform stream in the $x-z$ plane with a prescribed velocity jump $U(y,z) - U_\infty$ across the propeller disk.

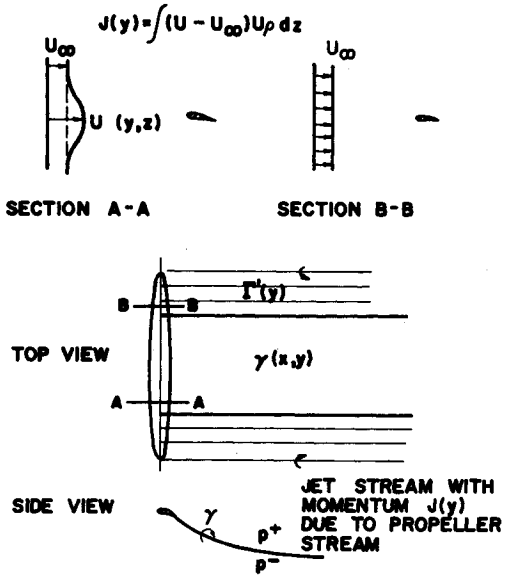

Fig. 4 Proposed scheme for the multipropeller (with propeller radius smaller than chord).

Equations (9–13) are the governing equations for the wing and multipropeller interference problem. The points inherent in Prandtl's theory hold also in the present formulation. In addition the following remarks will be made:

a) The governing equations involve only three functions $C(y)$, $J(y)$ and $C_L(y,\alpha)$ which are specified by the data of the wing and the propeller streams.

b) Similar to Prandtl's theory, among all the geometries which specify the planform only the chord distribution $C(y)$ will influence the solution. The influence of the detail geometry of the airfoil section appears implicitly through the lift coefficient C_L.

c) Only the integral $J(y)$ of the momentum gain across the propeller disks appears explicitly in the governing equations. The influences of the details of the velocity distribution behind the propeller streams and the locations of the propeller disks and the propeller axes appear implicitly through the sectional lift coefficient C_L.

d) The determination of the sectional lift coefficient $C_L(y,\alpha)$ is a tedious two-dimensional rotational flow problem. For propellers placed at a few chord length ahead of the leading edge of the wing, the influence of the wing on the velocity distribution behind the propeller can be ignored. The velocity distribution behind the propeller disk can be prescribed as the upstream condition in the analyses of the flow around the airfoil section and the analyses can be carried out by the numerical programs in Ref. 9 and 10. Some examples of the analyses are presented in Figs. 2 and 3 showing the variations of C_L. When propeller disks are within a fraction of the chord length ahead of the leading edge or behind the trailing edge or are in the middle of the wing, the finite difference program[10] for the calculation of C_L has to be modified to handle a prescribed jump of momentum across the propeller disk.

It was shown by Friedrichs[13] that Prandtl's lifting line theory can be rederived systematically by an asymptotic expansion with respect to the chord to span ratio. Equations (3) and (4) become the equations for the leading outer and inner solutions and Eq. (5) is the matching condition. In Van Dyke's formulation,[14] an additional assumption that the wing is thin and at a small angle of attack is imposed and explicit solutions are obtained.

In the next section the method of asymptotic expansion and matching will be employed to rederive in a systematic manner the governing equations presented in this section for the wing and multipropeller interference problem. In order to allow for finite disturbances in the local sectional analysis, the assumption of a thin airfoil will not be imposed and the analyses in the next section will proceed in the same manner as in Friedrichs' formulation.[13]

Systematic Formulation of the Wing and Multipropeller Interference Problem

For a wing with multipropellers, the location of a propeller disk x_p and the height of the stream behind the propeller are of the order of the midchord C_0, while the spanwise spread K of the combined propeller streams can be of the order of the span $2S$. The spanwise scale can be either K or S. The vertical and the streamwise length scale can be either the propeller radius or the midchord C_0. Near each propeller disk, the flowfield has another length scale b which is the chord of a propeller blade. Since the chord of a propeller blade is much smaller than that of a wing, details across the propeller disk can be ignored in the limit of $b/C_0 \to 0$. For the undisturbed flow, i.e., in absence of the wing, there is a uniform flowfield of velocity U_∞ ahead of the propeller disks and a nonuniform parallel stream behind them. The undisturbed velocity can be written as

$$\mathbf{v}(\bar{x},\bar{y},\bar{z}) = U_\infty \mathbf{i} \quad \text{for} \quad \bar{x} < x_p/C_0 \tag{14a}$$

$$= \mathbf{i}U(\bar{y},\bar{z}) \quad \text{for} \quad \bar{x} > x_p/C_0 \tag{14b}$$

where $\bar{x} = x/C_0$ and $\mathbf{i}$ is the unit vector along the x axis and the independent variables are nondimensionalized by the appropriate length scales for the propeller streams. To illustrate the effect of scaling in the limit of $\varepsilon = C_0/S \to 0$, the undisturbed velocity in the scale of S becomes

$$\mathbf{v}(\tilde{x},\tilde{y},\tilde{z}) = U_\infty \mathbf{i} \quad \text{for} \quad \tilde{x} < 0 \tag{15a}$$

$$= U_\infty \mathbf{i} \quad \text{for} \quad \tilde{x} > 0 \quad \text{except the cut along} \quad \tilde{z} = 0 \tag{15b}$$

where $\tilde{x} = \varepsilon\bar{x} = x/S$ and $\tilde{z} = z/S$. The property that $U(\tilde{y},\tilde{z}) \to U_\infty$ as $|\tilde{z}| \to \infty$ has been employed in converting Eq. (14b) to Eq. (15b). In order to balance the momentum, the gain in momentum across the propellers will now be concentrated in the cut. In other words the cut represents a thin sheet of jet with spanwise momentum distribution $J(\tilde{y})$ defined by the integral

$$J(\tilde{y}) = \rho C_0 \int_{-\infty}^{\infty} U(\tilde{y},\tilde{z})\left[U(\tilde{y},\tilde{z}) - U_\infty\right] d\tilde{z} \tag{16}$$

It should be pointed out here that the propeller disks may not be co-planar. In that case, an x_p has to be assigned for each propeller disk and Eqs. (14a, b) will be applied for each propeller disk. The differences between the x_p's will be important in the inner solution but they do not contribute to the leading terms in outer solutions for which x_p/S is equated to zero as indicated in Eqs. (15a, b)..

When the wing is present, the disturbance velocity will depend on the small parameter ε which is the ratio of the midchord to the half span, i.e.,

$$1 \gg \varepsilon = C_0/S \tag{17}$$

Because of the two different length scales C_0 and S, three different representations will be assumed for the three regions of the flowfield.

For the outer region, i.e., away from the wing and the propeller streams the disturbance velocity components $\tilde{u}$, $\tilde{v}$, $\tilde{w}$ and the disturbance pressure $\tilde{p}$ will be represented in the scale of the half span as follows

$$\tilde{u}(\tilde{x},\tilde{y},\tilde{z},\varepsilon) = \varepsilon\tilde{u}^{(1)}(\tilde{x},\tilde{y},\tilde{z}) + 0(\varepsilon) \tag{18a}$$

$$\tilde{v}(\tilde{x},\tilde{y},\tilde{z},\varepsilon) = \varepsilon\tilde{v}^{(1)}(\tilde{x},\tilde{y},\tilde{z}) + 0(\varepsilon) \tag{18b}$$

$$\tilde{w}(\tilde{x},\tilde{y},\tilde{z},\varepsilon) = \varepsilon\tilde{w}^{(1)}(\tilde{x},\tilde{y},\tilde{z}) + 0(\varepsilon) \tag{18c}$$

$$\tilde{p}(\tilde{x},\tilde{y},\tilde{z},\varepsilon) = \varepsilon\tilde{p}^{(1)}(\tilde{x},\tilde{y},\tilde{z}) + 0(\varepsilon) \tag{18d}$$

For the inner region, i.e., near the wing or the lifting line, the disturbance velocity components $\bar{u}$, $\bar{v}$, $\bar{w}$ and pressure $\bar{p}$ will be represented by scaling x and z variables with respect to the midchord as follows

$$\bar{u}(\bar{x},\tilde{y},\bar{z},\varepsilon) = \bar{u}^{(0)}(\bar{x},\tilde{y},\bar{z}) + 0(1) \tag{19a}$$

$$\bar{v}(\bar{x},\tilde{y},\bar{z},\varepsilon) = \varepsilon\bar{v}^{(1)}(\bar{x},\tilde{y},\bar{z}) + 0(\varepsilon) \tag{19b}$$

$$\bar{w}(\bar{x},\tilde{y},\bar{z},\varepsilon) = \bar{w}^{(0)}(\bar{x},\tilde{y},\bar{z}) + 0(1) \tag{19c}$$

$$\bar{p}(\bar{x},\tilde{y},\bar{z},\varepsilon) = \bar{p}^{(0)}(\bar{x},\tilde{y},\bar{z}) + 0(1) \tag{19d}$$

There is a third region where the variation in z direction is scaled by the midchord while the x and y variables are scaled by the half span to represent the disturbance velocity and the pressure inside the propeller streams. They are

$$\hat{u}(\tilde{x},\tilde{y},\bar{z},\varepsilon) = \hat{u}^{(0)}(\tilde{x},\tilde{y},\bar{z}) + 0(1) \tag{20a}$$

$$\hat{v}(\tilde{x},\tilde{y},\bar{z},\varepsilon) = \varepsilon\hat{v}^{(1)}(\tilde{x},\tilde{y},\bar{z}) + 0(\varepsilon) \tag{20b}$$

$$\hat{w}(\tilde{x},\tilde{y},\bar{z},\varepsilon) = \varepsilon\hat{w}^{(1)}(\tilde{x},\tilde{y},\bar{z}) + 0(\varepsilon) \tag{20c}$$

$$\hat{p}(\tilde{x},\tilde{y},\bar{z},\varepsilon) = \varepsilon\hat{p}^{(1)}(\tilde{x},\tilde{y},\bar{z}) + 0(\varepsilon) \tag{20d}$$

The leading terms for different regions and different components are not the same. Their appropriate order of magnitude are guided by the physical intuitions in the development of the lifting line theory and the thin jet theory. For example, in the outer solution the disturbance quantities should vanish as $\varepsilon \to 0$ and in the inner solution the spanwise variation, and hence $\bar{v}$ are of higher order. Of course, the analysis can begin with the assumption of a power series expansion in ε for all the quantities without discarding a priori any term of the order unity and the systematic matching procedure[14] will yield the results for the leading terms in Eqs. (18–20). This is omitted here, so that full attention can be devoted to explain how to use the matching procedures to obtain the governing equations, some of which are

difficult to foresee in the preceeding section from the physical intuitions alone.

It should also be pointed out here that the flowfield is assumed to be incompressible, rotational and inviscid, therefore, the physical conditions are the matching of pressure, mass flux and inclination. There can be discontinuity in velocity across a stream surface.

Inner Solution

The analysis will begin with the inner region. Equations (18a–d) will be substituted to the Euler equations and the continuity equation and the coefficients of like powers of ε will be equated for each equation. The leading equations are

$$\bar{u}_{\bar{x}}^{(0)} + \bar{w}_{\bar{z}}^{(0)} = 0 \tag{21a}$$

$$\bar{u}^{(0)}\bar{u}_{\bar{x}}^{(0)} + \bar{w}^{(0)}\bar{u}_{\bar{z}}^{(0)} = -(1/\rho)\bar{p}_{\bar{x}}^{(0)} \tag{21b}$$

and

$$\bar{u}^{(0)}\bar{w}_{\bar{x}}^{(0)} + \bar{w}^{(0)}\bar{w}_{\bar{z}}^{(0)} = (-1/\rho)\bar{p}_{\bar{z}}^{(0)} \tag{21c}$$

This represents a two-dimensional rotational flow in the $x-z$ plane with $\tilde{y}$ as a parameter. They can be reduced to a single equation for the stream function $\bar{\psi}^{(0)}(\bar{x}, \tilde{y}, \bar{z})$ with $\bar{\psi}_{\bar{z}}^{(0)} = U(\tilde{y}, \bar{z}) + \bar{u}^{(0)}$ and $\bar{\psi}_{\bar{x}}^{(0)} = -\bar{w}^{(0)}$. The equation for $\bar{\psi}^{(0)}$ is

$$\bar{\psi}_{\bar{x}\bar{x}}^{(0)} + \bar{\psi}_{\bar{z}\bar{z}}^{(0)} = -\omega(\bar{\psi}^{(0)}) \quad \text{for} \quad \bar{x} > x_p/C_0 \tag{22a}$$

and

$$\bar{\psi}_{\bar{x}\bar{x}}^{(0)} + \bar{\psi}_{\bar{z}\bar{z}}^{(0)} = 0 \quad \text{for} \quad \bar{x} < x_p/C_0 \tag{22b}$$

where ω is the vorticity created behind the propellers and is a given function of stream function. In case that the propeller is a few chord lengths ahead of the wing ($x_p < 0$), the disturbance of the airfoil on the flowfield immediately behind the propeller disk ($x = x_p + 0$) can be ignored. A boundary condition at $x = x_p{}^+$ can be imposed,

$$\bar{\psi}^{(0)}(x_p{}^+/C_0, \tilde{y}, \bar{z}) = \int_0^{\bar{z}} U(\tilde{y}, \bar{z}')\, d\bar{z}' \tag{23a}$$

The ω-function in Eq. (22a) will now be implicitly related to $\bar{\psi}^{(0)}$ by the condition,

$$\omega(\bar{\psi}^{(0)}) = -U_{\bar{z}}(\tilde{y}, \bar{z}) \tag{23b}$$

With Eq. (23a, b) and the boundary condition on the airfoil, the nonlinear Eq. (22a) for the domain $\bar{x} > \bar{x}_p$ can be solved numerically by the numerical program in Ref. 10.

In general Eqs. (22a) and (22b) will be coupled by a jump condition across the propellers. Since Eqs. (22a, b) involve only two variables $\bar{x}$ and $\bar{z}$, their solution subjected to the boundary condition on the airfoil can be obtained by a modification of the existing finite difference program in Ref. 10.

From the local two-dimensional numerical analysis, the relation between the sectional lift coefficient $C_L(\tilde{y}, \alpha)$ and angle of attack α will be obtained and the sectional lift is

$$L(\tilde{y}, \alpha) = \tfrac{1}{2}\rho U_\infty{}^2 C(\tilde{y}) C_L(\tilde{y}, \alpha) \tag{24}$$

Third Region (the Propeller Streams behind the Wing)

For the third region, i.e., in the propeller streams, Eqs. (20a–d) are substituted into the continuity equation and the Euler equations and the coefficients of like powers of ε in each equation are equal to zero. The leading equations are

$$\hat{u}_{\tilde{x}}^{(0)} + \hat{w}_{\tilde{z}}^{(1)} = 0 \tag{25a}$$

$$(U + \hat{u}^{(0)})\hat{u}_{\tilde{x}}^{(0)} + \hat{w}^{(1)}(U + \hat{u}^{(0)})_{\tilde{z}} = 0 \tag{25b}$$

$$(U + \hat{u}^{(0)})\hat{v}_{\tilde{x}}^{(1)} + \hat{w}^{(1)}\hat{v}_{\tilde{z}}^{(1)} = -\hat{p}_{\tilde{y}}^{(1)}/\rho \tag{25c}$$

and

$$0 = \hat{p}_{\tilde{z}}^{(1)}/\rho \tag{25d}$$

Eq. (25d) implies $\hat{p}^{(1)}$ is independent of $\bar{z}$ and the matching conditions with the outer solution yields

$$\tilde{p}^{(1)}(\tilde{x}, \tilde{y}, \tilde{z} = 0^+) = \hat{p}^{(1)}(\tilde{x}, \tilde{y}) = \tilde{p}^{(1)}(\tilde{x}, \tilde{y}, \tilde{z} = 0^-) \tag{26}$$

Equation (26) says that the pressure is continuous to the order of ε at the plane $\tilde{z} = 0$. It will become obvious in the analysis for the outer region that $\tilde{p}^{(1)}$ is an odd function of $\tilde{z}$ and Eq. (26) yields

$$\hat{p}^{(1)} \equiv 0 \tag{27}$$

Elimination of $\hat{u}_{\tilde{x}}^{(0)}$ from Eqs. (25a, b) gives

$$\varepsilon\hat{\theta}_{\tilde{z}}^{(1)} = [\varepsilon\hat{w}^{(1)}/(U + \hat{u}^{(0)})]_{\tilde{z}} = 0$$

$\varepsilon\hat{\theta}^{(1)}$, which is the inclination of the stream line with respect to the $\tilde{x}-\tilde{y}$ plane, is now independent of $\bar{z}$. The conditions for the matching of the inclination $\hat{\theta}^{(1)}$ with the outer solution $\tilde{\theta}^{(1)}$ yield

$$\tilde{\theta}^{(1)}(\tilde{x}, \tilde{y}, \tilde{z} = 0^+) = \hat{\theta}^{(1)}(\tilde{x}, \tilde{y}) = \tilde{\theta}^{(1)}(\tilde{x}, \tilde{y}, \tilde{z} = 0^-) \tag{28}$$

Also Eqs. (25b and c) can be rewritten as

$$(U + \hat{u}^{(0)})_s = 0 \quad \text{and} \quad \hat{v}_s^{(1)} = 0 \tag{29}$$

where $\partial/\partial s$ is the derivative along a stream line in the $\tilde{x}-\bar{z}$ plane. With the stream function $\hat{\psi}^{(1)}$ defined by the integral

$$\hat{\psi}^{(1)}(\tilde{x}, \tilde{y}, \bar{z}) = \int_0^{\bar{z}} [U(\tilde{y}, \bar{z}) + \hat{u}^{(0)}(\tilde{x}, \tilde{y}, \bar{z})]\, d\bar{z} - \int_0^{\bar{x}} \hat{w}^{(1)}(\bar{x}, \tilde{y}, 0)\, d\bar{x} \tag{30}$$

Eqs. (29) and (30) imply that the velocity components $U + \hat{u}^{(0)}$ and $\hat{v}^{(1)}$ are functions of $\hat{\psi}^{(1)}$ and $\tilde{y}$ only. The integral of the momentum gain across the third region, which is an integral of $U + \hat{u}^{(0)} - U_\infty$ with respect to $\hat{\psi}^{(1)}$, is a function of $\tilde{y}$ only. By matching with the inner solution, i.e., $\hat{u}^{(0)}(\bar{x} \to 0^+, \tilde{y}, \bar{z}) = \bar{u}^{(0)}(\bar{x} \to \infty, \tilde{y}, \bar{z}) = 0$, the momentum integral across the third region is identified as the sectional momentum gain across a propeller disk

$$\rho C_0 \int_{-\infty}^{\infty} (U + \hat{u}^{(0)} - U_\infty)\, d\hat{\psi}^{(1)} = \rho C_0 \int_{-\infty}^{\infty} (U - U_\infty) U\, d\bar{z} = J(\tilde{y}) \tag{31}$$

Eqs. (28) and (31) confirms the standard thin jet sheet approximations that the inclination is constant across the sheet and the momentum integral is constant with respect to $\tilde{x}$.

The next order momentum equation in the $\bar{z}$ direction is

$$[(U + \hat{u}^{(0)})\hat{w}^{(1)}]_s = -\hat{p}_{\bar{z}}^{(2)}/\rho \tag{32}$$

The conditions for matching with the outer solution above and below the third region, i.e., $\bar{z} \to 0^+$ and 0^-, respectively, are

$$\lim_{\bar{z} \to \pm\infty} [p^{(2)}(\tilde{x}, \tilde{y}, \bar{z}) - \bar{z}\tilde{p}_{\tilde{z}}^{(1)}(\tilde{x}, \tilde{y}, 0^\pm)] = \tilde{p}^{(2)}(\tilde{x}, \tilde{y}, 0^\pm) \tag{33}$$

Similarly the matching of stream function $\varepsilon\hat{\psi}^{(1)}$ in the $\tilde{x}-\bar{z}$ plane with the outer solution gives

$$\lim_{\bar{z} \to \pm\infty} [\hat{\psi}^{(1)}(\tilde{x}, \tilde{y}, \bar{z}) - \bar{z}U_\infty] = \tilde{\psi}^{(1)}(\tilde{x}, \tilde{y}, 0^\pm) = 0 \tag{34}$$

For the first-order outer solution the $\tilde{z}$ component of the momentum equation yields $\rho U_\infty{}^2\tilde{\theta}_{\tilde{x}}^{(1)} = -\tilde{p}_{\tilde{z}}^{(1)}$ Equation (33) becomes

$$\lim_{z \to \pm\infty} [\hat{p}^{(2)}(\tilde{x}, \tilde{y}, \bar{z}) + \rho U_\infty{}^2 \bar{z}\tilde{\theta}_{\tilde{x}}^{(1)}(\tilde{x}, \tilde{y}, 0^\pm)] = \tilde{p}^{(2)}(\tilde{x}, \tilde{y}, 0^\pm) \tag{35}$$

With the aid of Eqs. (34, 35, and 31). The integration of Eq. (32) with respect to $\bar{z}$ across the third region becomes

$$\begin{aligned} \Delta\tilde{p}^{(2)} &= \tilde{p}^{(2)}(\tilde{x}, \tilde{y}, 0^+) - \tilde{p}^{(2)}(\tilde{x}, \tilde{y}, 0^-) \\ &= -\rho\tilde{\theta}_{\tilde{x}}^{(1)}(\tilde{x}, \tilde{y}) \int_{-\infty}^{\infty} [U + \hat{u}^{(0)} - U_\infty]\, d\hat{\psi}^{(1)} \\ &= -J(\tilde{y})\tilde{\theta}_{\tilde{x}}^{(1)}/C_0 \end{aligned} \tag{36}$$

When $\varepsilon^2\Delta\tilde{p}^{(2)}$ and $\varepsilon\hat{\theta}^{(1)}$ are identified as the pressure difference Δp and the inclination θ and the $\tilde{x}$ derivative is replaced by the x derivative times S, the last equation reconfirms the equation for the bending of a thin sheet of jet, i.e., Eq. (7) in the preceding section.

Outer Solution

For the outer region, i.e., away from the wing, $\tilde{x}^2 + \tilde{z}^2 \not\approx 0$, and away from the propeller streams, $\tilde{z} \not\approx 0$ when $\tilde{x} > 0$, the flowfield is irrotational because the upstream velocity is uniform. The disturbance velocity components can be related to the disturbance potential $\tilde{\phi}(\tilde{x}, \tilde{y}, \tilde{z}, \varepsilon)$ which fulfills the Laplace equation

$$\tilde{\phi}_{\tilde{x}\tilde{x}} + \tilde{\phi}_{\tilde{y}\tilde{y}} + \tilde{\phi}_{\tilde{z}\tilde{z}} = 0 \tag{37}$$

The disturbance pressure is related to the potential through the Bernoulli's equation

$$\tilde{p}/\rho + \tfrac{1}{2}(U\mathbf{i} + \nabla\tilde{\phi})^2 = \tfrac{1}{2}U_\infty{}^2 \tag{38}$$

Eqs. (37) and (38) are equivalent to the continuity and Euler equations. $\tilde{\phi}(\tilde{x},\tilde{y},\tilde{z},\varepsilon)$ will be expanded in a power series of ε as follows:

$$\tilde{\phi}(\tilde{x},\tilde{y},\tilde{z},\varepsilon)=\varepsilon\tilde{\phi}^{(1)}(\tilde{x},\tilde{y},\tilde{z})+\varepsilon^2\tilde{\phi}^{(2)}(\tilde{x},\tilde{y},\tilde{z})+\dots \quad (39)$$

The velocity components and the pressure in Eqs. (18a, b, c, d) are now related to $\tilde{\phi}^{(1)}$,

$$\tilde{u}^{(1)}=\tilde{\phi}_{\tilde{x}}^{(1)}/S,\quad \tilde{v}^{(1)}=\tilde{\phi}_{\tilde{y}}^{(1)}/S,\quad \tilde{w}^{(1)}=\tilde{\phi}_{\tilde{z}}^{(1)}/S \quad (40a)$$

and

$$\tilde{p}^{(1)}=-\rho U_\infty\tilde{\phi}_{\tilde{x}}^{(1)}/S \quad (40b)$$

The disturbance potential $\tilde{\phi}^{(1)}$ fulfills also the Laplace equation. The solution of the equation is determined by specifying the singularities at $\tilde{x}^2+\tilde{z}^2=0$ and along $\tilde{z}=0$ with $\tilde{x}>0$ to match with the inner solution and the solution in the third region, respectively.

The matching of pressure with the inner solution or rather the matching of its integral, the sectional lift force $L(y,\alpha)$ given by Eq. (24), implies that there is a circulation distribution $\Gamma(\tilde{y})$ along the $\tilde{y}$ axis, the lifting line, such that the sectional lifting force is $L(\tilde{y},\alpha)$, i.e.,

$$\Gamma(\tilde{y})=L(\tilde{y},\alpha)/(\rho U_\infty)=\tfrac{1}{2}U_\infty C(\tilde{y})C_L(\tilde{y},\alpha)\quad\text{for}\quad|\tilde{y}|<1 \quad (41)$$

The variation of $\Gamma(\tilde{y})$ requires a vortex sheet extending downstream behind the lifting line with linear strength $\Gamma'(\tilde{y})/S$. This is the vortex system in the well known lifting line theory (see Fig. 4).

As a result of matching with the solution in the third region, Eqs. (26) and (28) imply that there is no discontinuity in pressure and inclination across the third region or that $\tilde{p}^{(1)}$ and $\tilde{\theta}^{(1)}$ are continuous across the trailing wake in the outer solution. Therefore, for the first-order outer solution, $\tilde{\phi}^{(1)}$, the solution in the third region does not create any singularity in addition to that of the lifting line.

First-Order Theory— Simplified Theory

Based only on the leading governing equations in the three regions and their matching conditions, a simplified theory is created. The inclination $\tilde{\theta}^{(1)}$ in the outer solution at the lifting line is related to the circulation distribution $\Gamma(y)$

$$\varepsilon\tilde{\theta}^{(1)}(\tilde{x}=0,\tilde{y},\tilde{z}=0)=\frac{1}{4\pi U_\infty S}\int_{-1}^{1}\frac{\Gamma'(\eta)\,d\eta}{\tilde{y}-\eta} \quad (42)$$

By matching with the inner solution, the effective angle of attack α in equation $C_L(\tilde{y},\alpha)$ is the related to the geometrical angle of attack $\alpha_g(\tilde{y})$, $\alpha(\tilde{y})=\alpha_g(\tilde{y})-\varepsilon\tilde{\theta}^{(1)}(0,\tilde{y},0)$ and Eq. (41) becomes

$$\Gamma(\tilde{y})=\tfrac{1}{2}U_\infty C(\tilde{y})C_L(\tilde{y},\alpha_g-\varepsilon\tilde{\theta}^{(1)}) \quad (43)$$

Equations (42) and (43) are the governing equations for the simplified theory. The equations are identical to the classical lifting line theory except that the lift coefficient $C_L(\tilde{y},\alpha)$ for the airfoil section inside the propeller stream is computed from the two-dimensional analysis of airfoil in a nonuniform parallel stream. In other words, the effect of propellers enters into the simplified theory implicitly by the change in the sectional lift coefficient due to the nonuniform velocity distribution behind the propellers.

Since the simplified theory is a first-order theory, the error decreases as $\varepsilon\to 0$ or $AR\to\infty$ provided the sectional momentum gain $J(\tilde{y})$ across the propellers is finite because terms proportional to $J(\tilde{y})$ will appear in the second-order theory. It is well known that the lifting line theory, which is formulated mathematically for a large aspect ratio, is quite accurate even for moderate aspects ratio as low as 2. Therefore, in the extension of the first-order theory to the second-order theory, only the contribution from the propeller streams which will be shown to be proportional to $\varepsilon^2 J^*$ where J^* is the propeller momentum parameter defined as

$$J^*=\max J(\tilde{y})/(\rho U_\infty{}^2C_0)=\max\int_{-\infty}^{\infty}\frac{U}{U_\infty}\left(\frac{U}{U_\infty}-1\right)dz \quad (44)$$

The accuracy of the simplified theory for moderate aspect ratio depends therefore also on the propeller momentum parameter J^*. For a given ε, the accuracy increases as J^* decreases. This prediction will be confirmed by the numerical examples to be presented later.

Systematic Theory

Prior to improving the first-order theory, it should be pointed out that the first-order solution $\tilde{\phi}^{(1)}$ is an odd function of $\tilde{z}$, and Eq. (40a, b) together with Eq. (26) yields

$$\tilde{u}^{(1)}(\tilde{x}>0,\tilde{y},0^{\pm})=0=\tilde{p}^{(1)}(\tilde{x}>0,\tilde{y},0^{\pm}) \quad (45a)$$

This result was employed to get Eq. (27). It should be noted that although $\tilde{\phi}_{\tilde{y}}^{(1)}$ or $\tilde{v}^{(1)}$ is also an odd function of $\tilde{z}$, $\tilde{v}^{(1)}$ is discontinuous across the sheet $\tilde{z}=0$. The value of $\tilde{v}^{(1)}$ above and below the sheet differ only in sign, therefore, $[\tilde{v}^{(1)}]^2$ is continuous across the sheet, i.e.,

$$[\tilde{v}^{(1)}(\tilde{x},\tilde{y},0^+)]^2=[\tilde{v}^{(1)}(\tilde{x},\tilde{y},0^-)]^2 \quad (45b)$$

with $\tilde{p}^{(1)}=0$ above and below the sheet, the Bernoulli's equation for $\tilde{z}=0^{\pm}$ becomes

$$\tilde{p}^{(2)}=-\rho U_\infty\tilde{u}^{(2)}-\tfrac{1}{2}\rho[(\tilde{v}^{(1)})^2+(\tilde{w}^{(1)})^2] \quad (46)$$

Since $\tilde{\theta}^{(1)}$, $\tilde{w}^{(1)}$ and $(\tilde{v}^{(1)})^2$ are continuous across the sheet, Eqs. (46) and (36) yield

$$\tilde{u}^{(2)}(\tilde{x}>0,\tilde{y},0^+)-\tilde{u}^{(2)}(\tilde{x}>0,\tilde{y},0^-)=-J(\tilde{y})\tilde{\theta}_{\tilde{x}}^{(1)}(\tilde{x},\tilde{y})/(\rho U_\infty C_0)$$

This discontinuity in $\tilde{u}$ is equivalent to a vorticity distribution $\tilde{\gamma}(\tilde{x},\tilde{y})j$ on the $\tilde{x}$–$\tilde{y}$ plane with

$$\tilde{\gamma}(\tilde{x},\tilde{y})=\varepsilon^2\tilde{\gamma}^{(2)}(\tilde{x},\tilde{y})=-J(\tilde{y})\varepsilon\tilde{\theta}_{\tilde{x}}^{(1)}(\tilde{x},\tilde{y})/(\rho U_\infty S)\quad\text{for}\quad\tilde{x}>0 \quad (47)$$

The momentum gain, $J(\tilde{y})$, across the propeller disks has to adjust to the inclination $\varepsilon\tilde{\theta}^{(1)}(0,\tilde{y},0)$. This change in momentum requires a sectional vertical force of the magnitude $\varepsilon J\tilde{\theta}^{(1)}$. To account for this sectional force for the outer solution there should be a circulation distribution $\Gamma_J(\tilde{y})$ along the $\tilde{y}$ axis with

$$\rho U_\infty\Gamma_J(\tilde{y})=-J\varepsilon\tilde{\theta}^{(1)}(0,\tilde{y},0) \quad (48)$$

The system of singularities in the outer solution is now composed of a lifting line with a circulation distribution $\Gamma(\tilde{y})$ for the lift on the wing and another distribution $\Gamma_J(\tilde{y})$ to deflect the momentum of the propeller streams and a trailing surface with a vorticity distribution $\gamma(\tilde{x},\tilde{y})\mathbf{j}$. The inclination induced by this vortex system is

$$\tilde{\theta}(\tilde{x},\tilde{y},\tilde{z})=\int_{-1}^{1}G(\tilde{x},\tilde{y}-\eta,\tilde{z})\Gamma'(\eta)\,d\eta+\int_{-\infty}^{\infty}G(\tilde{x},\tilde{y}-\eta,\tilde{z})\Gamma_J'(\eta)\,d\eta+\int_0^{\infty}d\xi\int_{-\infty}^{\infty}d\eta\,G(\tilde{x}-\xi,\tilde{y}-\eta,\tilde{z})\gamma(\xi,\eta) \quad (49)$$

where

$$G(\xi,\eta)=\frac{1}{4\pi U_\infty S}\left\{\frac{\tilde{y}}{\tilde{y}^2+\tilde{z}^2}+\frac{\tilde{x}\tilde{y}}{(\tilde{x}^2+\tilde{y}^2+\tilde{z}^2)^{1/2}}\times\left[\frac{1}{\tilde{x}^2+\tilde{z}^2}+\frac{1}{\tilde{y}^2+\tilde{z}^2}\right]\right\}$$

The spanwise integrations for the second and the third integrals are carried over the interval where $J(\eta)\neq 0$. Equations (43) and (48) provide the relation between $\tilde{\theta}$, Γ and Γ_J. They are

$$\Gamma(\tilde{y})=\tfrac{1}{2}U_\infty C(\tilde{y})C_L(\tilde{y},\alpha_g-\tilde{\theta}(0,\tilde{y},0)) \quad (50)$$

and

$$\Gamma_J(\tilde{y})=-J(y)\tilde{\theta}(0,\tilde{y},0)/(\rho U_\infty) \quad (51)$$

With $\tilde{\theta}$ defined by Eq. (49), Eqs. (47, 50, and 51) are the governing equations for $\tilde{\gamma}$, Γ and Γ_J. These equations concur with Eqs. (9–13) presented in the preceding section.

It should be pointed out here that the last two integrals in Eq. (49) are the second-order terms added to $\varepsilon\tilde{\theta}^{(1)}$. The appear-

ance of $\tilde{y}$ and Γ_J in the integrands causes the coupling of Eq. (50) with Eqs. (47) and (51). $\tilde{\gamma}(\tilde{x},\tilde{y})$ and $\Gamma_J(\tilde{y})$ represent the contribution of the propeller streams to the vortex system of the outer solution. They also account for the difference between the present analysis and the simplified analysis. Their order of magnitude as compared to the basic vortex system of the wing $\Gamma(\tilde{y})$ can be obtained from Eqs. (47, 50, and 51). The results are

$$\Gamma_J(\tilde{y})/\Gamma(\tilde{y}) = 0(J^*\varepsilon) \quad \text{and} \quad S\tilde{\gamma}(\tilde{x},\tilde{y})/\Gamma(\tilde{y}) = 0(J^*\varepsilon) \tag{52}$$

where J^* is the propeller momentum parameter defined in Eq. (44).

For a wing of moderate aspect ratio, ε can be of the order of $\frac{1}{2}$ while J^* can be of the order of 2 or higher during takeoff, therefore, $J^*\varepsilon$ will not be small and the contributions of Γ_J and $\tilde{\gamma}$ may produce significant difference between the present analysis and the simplified analysis. Their differences will be demonstrated by the numerical examples in the next section.

Numerical Solutions and Examples

In order to avoid numerical evaluation of the derivative of $\tilde{\theta}$ with respect to $\tilde{x}$ in Eq. (47), the equation will be integrated with respect to $\tilde{x}$. The result is

$$\int_0^{\tilde{x}} \tilde{\gamma}(\tilde{x},\tilde{y})\,d\tilde{x} = J(\tilde{y})\,[\tilde{\theta}(0,\tilde{y},0) - \tilde{\theta}(\tilde{x},\tilde{y},0)]/(\rho U_\infty S) \quad \text{for } \tilde{x} > 0 \tag{53}$$

Equation (53), together with Eqs. (50) and (51) will be the governing equations for Γ, Γ_J and $\tilde{\gamma}$. These equations will be supplemented by the following boundary conditions

$$\Gamma(\tilde{y}) = 0 \quad \text{at} \quad \tilde{y} = \pm 1 \tag{54a}$$

$$\Gamma_J(\tilde{y}) = 0 \quad \text{and} \quad \tilde{\gamma}(\tilde{x},\tilde{y}) = 0 \quad \text{when} \quad J(\tilde{y}) = 0 \tag{54b}$$

and

$$\tilde{\gamma}(\tilde{x} \to \infty, \tilde{y}) = o(\tilde{x}^{-1}) \tag{54c}$$

The first two equations insure the spanwise continuity of pressure at the wing tips and at the edges of the thin sheet of propeller streams. The last condition is imposed so that the integral in Eq. (53) has a limit as $\tilde{x} \to \infty$.

For the simplified theory, the governing equations, Eqs. (42), and (43), are identified to those in the lifting line theory with a prescribed lift coefficient $C_L(\tilde{y},\alpha)$, therefore, the numerical solutions can be obtained by Glauert's method.[15]

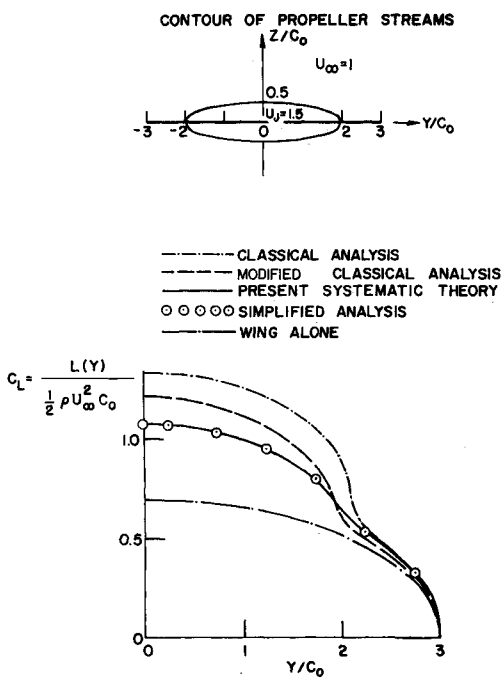

Fig. 5 Spanwise lift distribution with overlapping multipropellers with low-momentum gain ($J^* = 0.75$, $\varepsilon = \frac{1}{3}$).

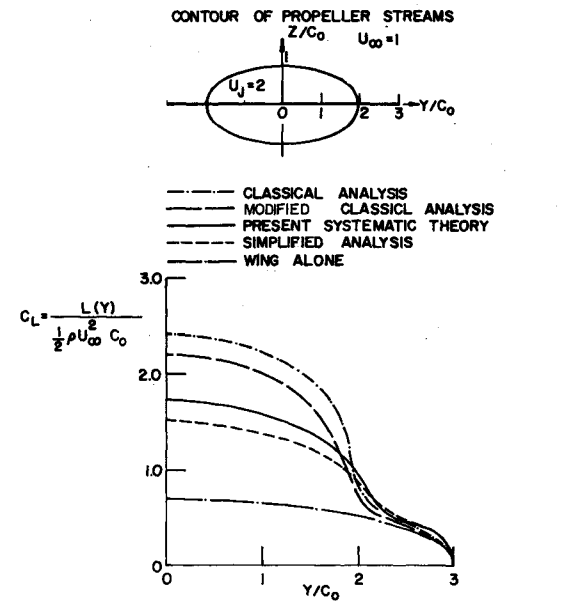

Fig. 6 Spanwise lift distribution with overlapping multipropellers with high momentum ($J^* = 4$, $\varepsilon = \frac{1}{3}$).

For the systematic theory, the numerical solutions of Eqs. (53, 50, and 51) will be obtained by a method similar to that in the lifting surface theory.[15] $\Gamma(\tilde{y})$ and $\Gamma_J(\tilde{y})$ will be represented by polynomials of $\tilde{y}$. The surface distribution $\tilde{\gamma}(\tilde{x},\tilde{y})$ is replaced by discrete horseshoe vortices of strength $\Gamma_i(\tilde{y}) = \tilde{\gamma}\Delta\tilde{x}$ located along $\tilde{x}_i = i(\Delta\tilde{x})$. Each $\Gamma_i(\tilde{y})$ will also be represented by a polynomial of $\tilde{y}$. These polynomials will fulfill the boundary conditions of Eqs. (54a, b, c). The unknown coefficients in the polynomials of $\Gamma(\tilde{y})$, $\Gamma_J(\tilde{y})$ and $\Gamma_1(\tilde{y})$, $\Gamma_2(\tilde{y})\ldots$ are determined by a system of algebraic equations obtained by fulfilling Eqs. (53, 50, and 51) at a discrete set of points. Details for this numerical analysis are described in Ref. 6.

It has been emphasized in the preceding sections that the location of the propellers relative to the wing and the detail velocity distribution $U(y,z)$ behind the propeller disks influence the solution only through sectional lift coefficient $C_L(y,\alpha)$. Since the search for the wing and multipropeller interference experiments, which provides also a survey of the detail velocity distribution $U(y,z)$, has not been successful and it is time consuming to compute C_L for an airfoil in a nonuniform stream, the numerical examples in this paper will make use of the available C_L functions computed for special airfoil sections in nonuniform streams as shown in Figs. 2 and 3. Although in these computations the nonuniform velocity profile is prescribed as the upstream condition, the application of these C_L functions to the present problem is consistent with the Prandtl's hypothesis, i.e., the matching of the outer solution in the scale of span near the lifting line with the inner solution at a distance large relative to the chord. In practice, the C_L functions can be used as good approximations for the propeller disks placed at one or two chord distances ahead of the leading edge. In this case, the position of the propeller disk does not appear in the problem except in the sense that its distance x_p from the lifting line be large enough that Figs. 2 and 3 apply but small compared to the span.

The C_L functions in Fig. 2 are employed for the numerical examples in Figs. 5 to 8. The wing is a flat plate with elliptical planform with $S/C_0 = 3$. The geometrical angle of attack is 8°. In each figure, the cross section of the propeller streams is shown. The sectional height is $2h(y)$. The velocity U_J inside is uniform. For each ratio of U_J/U_∞, 1.5 or 2, the C_L/α curve in Fig. 2 is a known function of $h(y)/C(y)$.

The contours of the propeller streams in Figs. 5 and 6 are ellipses with major axes equal to $2C_0$. The minor axis is $C_0/2$

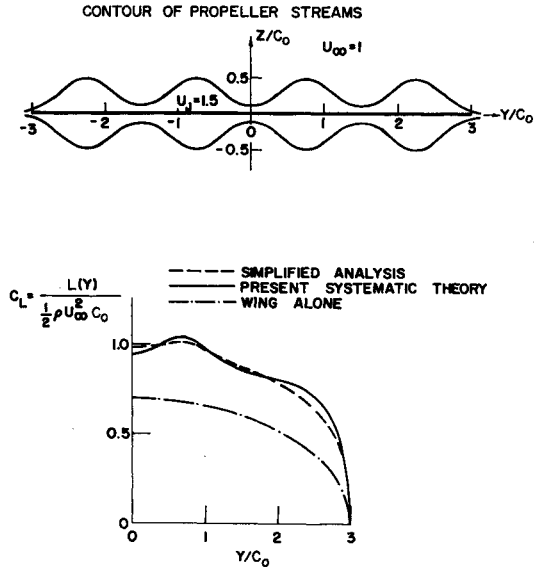

Fig. 7 Spanwise lift distribution with four propellers with low-momentum gain across propeller ($J^* = 0.75$, $\varepsilon = \frac{1}{3}$).

in Fig. 5 and C_0 in Fig. 6. The velocity ratio U_J/U_∞ is 1.5 in Fig. 5 and 2 in Fig. 6. It is clear in Fig. 5 that the spanwise lift distribution given by the simplified analysis is very close to that of the systematic theory since the momentum parameter J^* is 0.75. In Fig. 6 the result of the result of the simplified analysis is less satisfactory because of the larger J^* which equals to 4. For the special case that the contour of the propeller streams is an ellipse, the classical analysis has been adapted to generalize the circular contour in the assumption 1 to an ellipse.[6,7] Curves labeled "classical analysis" in Figs. 5 and 6 are obtained without any modification to the assumption 4, i.e., the values for C_L outside and inside the propeller stream at $2\pi\alpha$ and $2\pi\alpha(U_J/U_\infty)^2$, respectively. The "classical analysis" is therefore an extension of the Koning's theory[2] to propeller streams of elliptical contour by the method of conformed mapping.[6,7] For the curves labeled "modified classical analysis" the assumption 4 in the classical analysis is modified so that the C_L function is related to the sectional height of the propeller stream as given by the curves in Fig. 2.

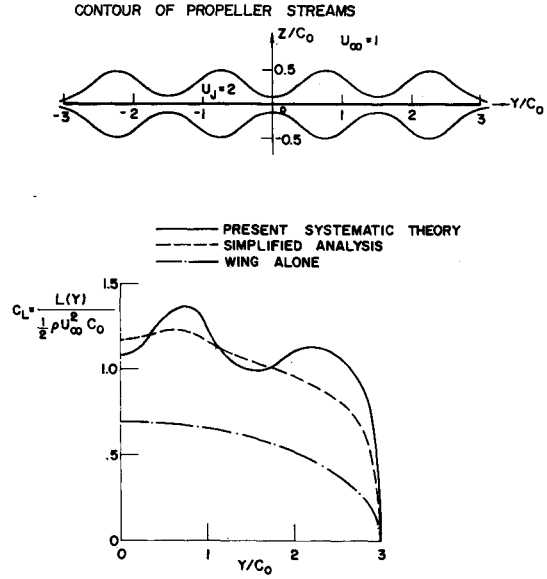

Fig. 8 Spanwise lift distribution with four propellers with high-momentum gain across propeller ($J^* = 2$, $\varepsilon = \frac{1}{3}$).

The "modified classical analysis" is an extension of the analysis in Ref. 12 for the propeller streams with a circular contour to those with an elliptical contour and is described in detail in Sec. II-B1 of Ref. 6 and in Sec. 2 of Ref. 7. Although the modified classical analysis, the simplified analysis and the systematic theory employ the same sectional lift to angle-of-attack relationship $L(y,\alpha)$ given by Fig. 2, they differ in the three-dimensional vortex systems. In the modified classical analysis, the circulation $\Gamma(y)$ is $L(y,\alpha)/(\rho U_J)$ and $L(y,\alpha)/(\rho U_\infty)$, respectively, for the wing section inside and outside the propeller streams. In addition there are additional vortex systems to fulfill the boundary conditions across the interface between the propeller and the outer streams. In the simplified analysis, the circulation $\Gamma(y)$ is $L(y,\alpha)/(\rho U_\infty)$ for the entire lifting line and there is no additional vortex systems. The systematic theory differs from the simplified theory by the additional vortex systems due to the bending of the thin sheet of the propeller streams.

In both Figs. 5 and 6, the spanwise lift distribution of the "classical analysis" is higher than that of the "modified classical analysis." The difference represents the effect of the finite sectional height of the propeller streams. In both figures the lift curve given by the modified classical analysis is higher than that of the systematic analysis and also the simplified analysis. The difference shows that the effect of extending the propeller streams to upstream infinity relative to the span in both the classical analysis and the modified classical analysis.

Figures 7 and 8 show the spanwise lift distribution with four propellers. The contours for the propeller streams are the same in both figures. The velocity U_J inside the stream is $1.5\,U_\infty$ in Fig. 7 and $2\,U_\infty$ in Fig. 8. In Fig. 7, the propeller momentum parameter is smaller ($J^* = 0.75$) and there is good agreement between the simplified and the systematic analysis. In Fig. 8, the parameter is larger ($J^* = 2$) and the difference between the simplified and the systematic analysis is slight but noticeable.

Figure 9 shows the application of the present analysis for the case that the velocity distribution $U(y,z)$ behind the propeller streams is nonuniform and merges continuous into the outer uniform velocity U_∞. In order to make use of the C_L given in Fig. 3, the airfoil section is the same Joukowski profile described in the introduction for Fig. 3. The planform is again elliptic with $S/C_0 = 3$. The geometrical angle of attack is 4°. The nonuniform velocity distribution is assumed to be

$$U(y,z)/U_\infty = 1+\exp\{-(1.81)^2[(y-1.5C_0)^2+z^2]/C^2\}+ \exp\{-(1.81)^2[(y+1.5C_0)^2+z^2]/C^2\} \qquad (55)$$

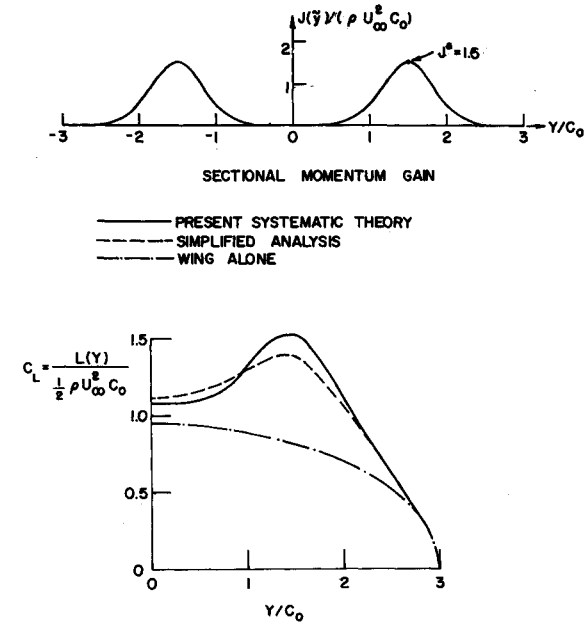

Fig. 9 Spanwise lift distribution with two propellers with nonuniform velocity distribution given by Eq. (55).

so that at each station y, the velocity profile is given by the same function of z specified in Fig. 3. The coefficient $a(y)$ in Eqs. (1) is identified as

$$a(y) = \exp\{-[1.81(y-1.5C_0)/C]^2\} + \exp\{-[1.81(y+1.5C_0)/C]^2\} \quad (56)$$

The velocity distribution in Eq. (55) simulates that of two propeller streams with axes located at $y = \pm 1.5C_0$ and $z = 0$. In the present case, a boundary for the propeller streams is not defined. Figure 9 shows the spanwise variation of the momentum integral $J(y)$. With the dependence of C_L on $a(y)$ and α given by Fig. 3 and with $a(y)$ defined by Eq. (56), computations for the spanwise lift distribution are carried out. Figure 9 shows that, with a moderate J^* of 1.5, there is a slight difference between the simplified and the systematic analyses.

Conclusions

Based on the fact that the radii of the propellers are of the order of the chord and are much smaller than the span, a systematic analysis with the chord to span ratio as the expansion parameter is presented. The analysis is very versatile. The same scheme can handle either overlapping or non-overlapping multipropellers without any restriction to the contour of the propeller streams and to the velocity profile behind the propellers. These statements are demonstrated by the examples in Figs. 5 to 9.

A change in the velocity distribution behind the propellers or a change in the location of the propeller disks (whether ahead, behind or in the middle of the wing) can be handled by the same scheme with only a modification of the sectional two-dimensional analysis for the determination of a new C_L function.

For the special case that the overlapping propeller streams have an elliptical contour and a uniform velocity, the classical theory can be adapted to carry out some analyses. The numerical results in Figs. 5 and 6 show that the classical analysis overestimates the influence of the propellers because of the use of too large C_L for the section inside the propeller streams and of the extension of the propeller streams to upstream infinity in the scale of the span.

From the systematic analysis, a simplified theory is obtained which includes the effect of propeller stream on the sectional lift coefficient in the local two-dimensional analysis but ignores the equivalent vortex system of the propeller streams in the global three-dimensional analysis. This simplified analysis is quite accurate when the propeller momentum parameter J^* defined by Eq. (44) is less than unity.

The analysis presented in this paper can be applied directly to the interference of wing with multiple jets.

References

[1] Ferrari, C., "Propeller and Wing Interactions at Subsonic Speeds," *Aerodynamic Components of Aircraft at High Speed*, edited by A. F. Donovan and H. C. Lawrence, Princeton University Press, Princeton, N.J., 1957, Sec. C, Chap. 3,

[2] Koning, C., "Influence of the Propeller on Other Parts of the Airplane Structure," *Aerodynamic Theory*, Div. M, Vol. IV, edited by W. F. Durand, Springer-Verlag, Berlin, 1935; also Dover, New York, 1963.

[3] von Kármán, Th. and Burgers, J. M., "General Aerodynamic Theory-Perfect Fluids," *Aerodynamic Theory*, Div. E, Vol. II, edited by W. F. Durand, Springer-Verlag, Berlin, 1935; also Dover, New York, 1963.

[4] Rethorst, S., "Aerodynamics of Nonuniform Flows as Related to an Airfoil Extending Through a Circular Jet," *Journal of the Aeronautical Sciences*, Vol. 25, No. 1, Jan. 1958, pp. 11–28.

[5] Wu, T. Y. and Talmadge, R. B., "A Lifting Surface Theory for Wings Extending Through Multiple Jets," Rept. 8, Aug. 1961, Vehicle Research Corp., Pasadena, Calif.

[6] Liu, C. H., "Interference for Wing with Single and with Multi-Propellers," Ph.D. thesis, Aug. 1971, New York Univ., School of Engineering and Science, Bronx, N.Y.

[7] Ting, L., Liu, C. H., and Kleinstein, G., "Interference of Wing and Multi-Propellers," NYU Rept. AA-71-13, June 1971, New York Univ., Bronx, New York; also, AIAA Paper 71-614, Palo Alto, Calif., 1971.

[8] Muskhelishvili, N. I., *Some Basic Problems of the Mathematical Theory of Elasticity*, P. Noordhoff Ltd., Groningen-Holland, 1953.

[9] Jameson, A., "Analysis of Wing Slipstream Flow Interaction," CR-1632, Aug. 1970, NASA.

[10] Ting, L. and Liu, C. H., "Thin Airfoil in Nonuniform Parallel Streams," NYU Rept. AA-68-20, July 1968, New York Univ., Bronx, N.Y.

[11] Chow, F., Krause, E., Liu, C. H., and Mao, J., "Numerical Investigations of an Airfoil in a Nonuniform Stream," *Journal of Aircraft*, Vol. 7, No. 6, Nov.–Dec. 1970, pp. 531–537.

[12] Kleinstein, G. and Liu, C. H., "Application of Airfoil Theory for Nonuniform Streams to Wing Propeller Interaction," Rept. AA-71-06, March 1971, New York Univ.; also *Journal of Aircraft*, Vol. 9, No. 2, Feb. 1972, pp. 137–142.

[13] Friedrichs, K. O., *Special Topics in Fluid Dynamics*, Gordon and Breach, Science, New York, 1966.

[14] Van Dyke, M. D., *Perturbation Methods in Fluid Mechanics*, Academic Press, New York, 1964.

[15] Robinson, A. and Laurmann, J. A., *Wing Theory*, Cambridge University Press, New York, 1956.